An innovative therapeutic approach for malignant mesothelioma treatment based on the use of Gd/boron multimodal probes for MRI guided BNCT

An innovative therapeutic approach for malignant mesothelioma treatment based on the use of Gd/Boron multimodal probes for MRI guided BNCT

Diego Alberti[a] *Annamaria Deagostino*[b], *Antonio Toppino*[b], *Nicoletta Protti*[c,d], *Silva Bortolussi*[c,d], *Saverio Altieri*[c,d], *Silvio Aime*[a,e], *Simonetta Geninatti Crich*[a*].

[a]*Department of Molecular Biotechnology and Health Sciences; University of Torino, via Nizza 52, Torino, 10126, Italy.*

[b]*Department of Chemistry, University of Torino, via Pietro Giuria 7, Torino, 10125, Italy;*

[c]*Department of Physics, University of Pavia, via Agostino Bassi 6, Pavia, 27100, Italy;*

[d]*Nuclear Physics National Institute (INFN), Unit of Pavia, via Agostino Bassi 6, Pavia, 27100, Italy.*

[e]*IBB-CNR, Sede Secondaria c/o MBC, via Nizza 52, 10126 Torino. Italy.*

Corresponding Author

*Simonetta Geninatti Crich,

Department of Molecular Biotechnology and Health Sciences,

University of Torino,

via Nizza 52, 10126, Torino (Italy);

email: **simonetta.geninatti@unito.it**

ORCID: orcid.org/0000-0003-2998-5424

ABSTRACT The aim of this study is to develop an innovative imaging guided approach based on Boron Neutron Capture Therapy, for the treatment of mesothelioma, assisted by the quantification of the *in vivo* boron distribution by MRI. The herein reported results demonstrate that overexpressed Low Density Lipoproteins receptors can be successfully exploited to deliver to mesothelioma cells a therapeutic dose of boron (26µg/g), significantly higher than in the surrounding tissue (3.5µg/g). Boron and Gd cells uptake was assessed by ICP-MS and MRI on two mesothelioma (ZL34, AE17) and two healthy (MRC−5 and NMuMg) cell lines. An *in vivo* model was prepared by subcutaneous injection of ZL34 cells in Nu/Nu mice. After irradiation with thermal neutrons, tumor growth was evaluated for 40 days by MRI. Tumor masses of boron treated mice showed a drastic reduction of about 80-85%. The obtained results appear very promising providing patients affected by this rare disease with an improved therapeutic option, exploiting LDL transporters.

KEYWORDS Mesothelioma, Boron Neutron Capture Therapy, Magnetic Resonance Imaging (MRI), Low Density Lipoproteins.

1. INTRODUCTION

Malignant Mesothelioma (MM) is an aggressive tumor with a poor prognosis whose incidence and mortality is a function of past exposure to asbestos, even after a latency period of 30-50 years. MM is recognized as a rare occupational disease lacking of any significant therapies and the median survival after diagnosis is less than 9-12 months[1,2]. MM is a disseminated tumor, spreading inside the whole pleura or peritoneum. Conventional radiotherapies have limited effectiveness due to the presence of several radiosensitive tissues, which limit the maximum dose deliverable to the malignant nodules. Targeted therapies represent one of the major focus of cancer research today and many future advances in cancer treatment are expected to come from this approach. However, an effective therapy based on molecular-targeting against MM does not exist yet because of the lack of knowledge of highly specific MM biomarkers. The absence of MM biomarkers also reduces the possibility to perform an early diagnosis of MM that remains a challenge for the clinicians. In spite of the numerous studies aimed at finding suitable biomarkers in blood and pleural effusions, these efforts have not yet produced an effective diagnostic tool [3,4]. Herein we propose Low Density Lipoproteins (LDL) receptors as targets for the design of tailored “theranostic” agents. LDL are natural nanoparticles devoted to the transport of fats (triglicerids, cholesterol, cholesterol esters) within the body through the blood stream. While there are many examples of synthetic nanocarriers, optimized to deliver drugs or imaging probes to the pathological site [5], endogenous nano-systems have not yet received great attention in spite of the fact that, the use of biological nanoparticles could result largely advantageous because of their good tolerability, biodegradability and low immunogenity [6,7]. Moreover, it is possible to exploit their natural target receptors in particular when they are overexpressed by the pathologic tissue. The up-regulation of LDL receptors expression has been found in many aggressive tumors such us melanoma, glioma, breast cancer [8,9], but, to the best of our

knowledge, it has not been quantitatively determined in the case of mesothelioma. Thus, in this study, LDL receptors expression was assessed on two different mesothelioma cell lines. LDL have already been proposed as specific carriers for carboranes (icosahedral lipophilic clusters containing boron atoms) used as Boron Neutron Capture Therapy (BNCT) agents. BNCT is an example of targeted therapy with good efficacy and low toxicity that provides a tumor-selective cell death [10,11]. More specifically, this therapy is able to combine low energy thermal neutron irradiation with the presence of boron containing agents at the targeted pathological tissues. Neutrons are captured by non-radioactive ^{10}B yielding ^{11}B nuclei that disintegrate into alpha particles and lithium-7 causing not reparable damage specifically to the cell where they were produced, while sparing the surrounding healthy ones thanks to short ranges (few micrometers) of these charged particles in tissues. This property makes BNCT a promising treatment for diffused metastasis and infiltrating tumors as mesothelioma that cannot be treated by methods needing the presence of a localized tumor mass, such as conventional radiotherapy or surgery. Nakamura and coworkers recently developed a Hyaluronic acid containing BSH specifically delivered to MM in preclinical mouse models [12]. Moreover, a small number of MM patients were safely treated with BNCT in Japan in 2006, achieving a significant palliation of the symptoms [13]. BNCT selectivity, determined by the drug distribution in cells, allows the delivery of very high doses in the tumor tissues, significantly reducing the side effects in the healthy tissues. BNCT has been applied to skin melanoma, brain and head and neck tumors and a large amount of clinical data have been collected through the different clinical trials (I/II phase) carried out in Japan, USA, the Netherlands, Sweden, Finland, Argentina and Taiwan [14]. A rough estimation shows that approximately 800 patients (data acquired until 2012) have been treated with BNCT reporting around 50% of complete tumor-remission [15]. Several stringent

conditions have to be simultaneously respected: (i) low toxicity for normal cells for compounds to be used in BNCT: (ii) high selectivity for tumor cells; (iii) long half-life within the tumor; (iv) non-invasive triggering mechanisms for tumor destruction. It has been estimated that approximately 10-30 μg of boron per gram of tumor mass is needed to attain an effective treatment, using a tolerable irradiation time and a suitable neutron source [16]. The two compounds currently used in clinical trials are *L*-para-boronphenylalanine (BPA) (used in trials for glioblastoma, head and neck cancer and melanomas), and sodium mercaptoundecaidro-closo-dodecaborate (BSH) (designed for brain tumor treatments). These systems yield a boron concentration ratio between tumor and normal tissues in the range between 3 and 6 allowing a safe and quite effective treatment. However, it is a widespread opinion in the scientific community that a wider clinical application of BNCT will be possible when the uptake in targeting tumor cells will be further improved [16]. Accurate estimation of the BNCT dose is one of the others challenging issues in BNCT [17]. The dose estimation depends on the precise knowledge of thermal neutron flux and capture agent concentrations in tumor and normal tissues during neutron irradiation. A non-invasive, real time method to access to the measurements of the actual concentration of BNCT agents has not yet been used in clinical applications. To date, boron concentrations are measured in blood, and then extrapolated in tumor and normal tissues on the basis of biodistribution studies previously performed. However, boron distribution is expected to vary by different patients causing large uncertainties in the estimation of tumor-to-blood concentration ratio.

For these reasons, the herein proposed agent will be specifically designed to improve the specific uptake of boron and Gd ions in MM cells by conjugating carboranes cages with amphiphilic Gd-complexes. This dual MRI/BNCT probe, endowed with a high affinity for LDL will be

selectively targeted to MM cells, by exploiting the up regulation of their specific receptors. Several examples of functionalised carboranes were used to prepare boron delivery vehicles for BNCT, as they contain a high number of boron atoms and they are endowed with high stability *in vivo* [18−21]. The presence of Gd-complexes as MRI reporters allows the indirect quantitative determination of boron at the target site before and during neutron irradiation. The herein developed targeted agent (Figure 1, AT101) has been already tested on murine melanoma [22] and breast pulmonary metastasis [23] on preclinical mice models. It was able to deliver a therapy precisely tailored via its monitoring by *in vivo* MR imaging. This approach may open new therapeutic strategies for patients affected by MM, leading to better outcomes of the treatment, in terms of survival time and quality of life.

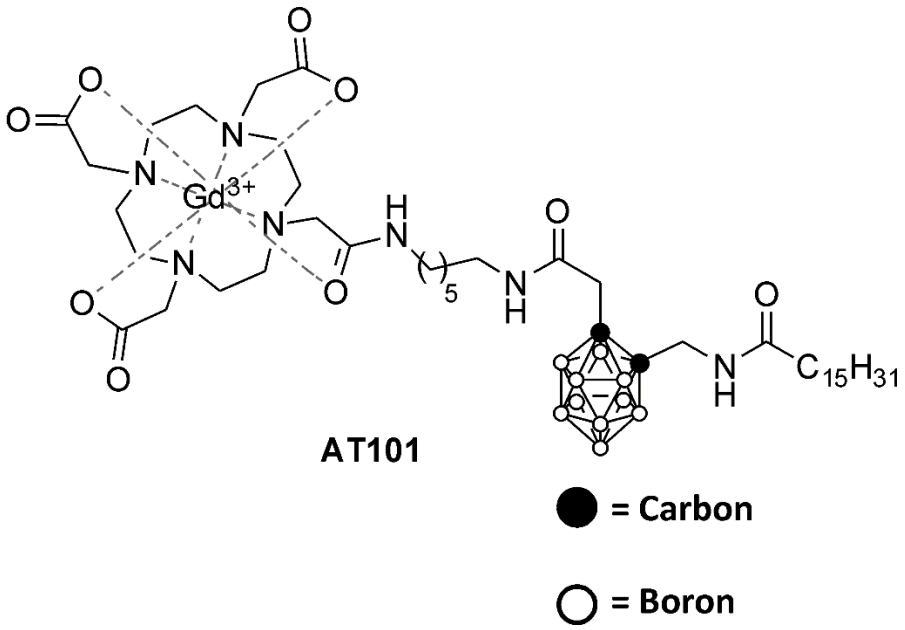

Figure 1: Schematic representation of the dual boron/Gd agent (AT101).

2. MATERIALS AND METHODS

The ^{10}B enriched ligand- C-[N-(DOTAMA-C6)-carbamoylmethyl]C′-palmitamidomethyl-o-carborane (^{10}B enriched AT101) was synthesized according to the previously reported procedure [24].

2.1 LDL Adducts Preparation. In water solution the aggregation of AT101 complex in micelles prevents its binding to LDL. For these reasons, an excess of β-cyclodextrin (β-CD) (25:1) was added to the 0.13 mM AT101 complex solution in order to disaggregate the micelles (15', 25°C). Then, AT101/ β-CD adduct (0.12 mM) was incubated in the presence of 0.36 μM LDL (Biomedical Technologies Inc., Stoughton, MA) for two hours at 37°C. After removing by dialysis β-CD and the unbound complex, LDL particles were loaded with 215±20 complexes and they were used for *in vitro* experiments. For *in vivo* experiments, AT101/LDL solution was also concentrated up 10 mM Gd by Vivaspin filters (Sartorius)(molecular weight cutoff = 10000). The final Gd concentration was measured by inductively coupled plasma mass spectrometry (ICP-MS) (Element-2; Thermo-Finnigan, Rodano (MI), Italy). AT101/LDL adducts mineralization was carried out with 1ml of concentrated HNO_3 (70%) under microwave heating for 20' at 160°C (Milestone MicroSYNTH Microwave labstation). Protein concentration was determined by a commercial Bradford assay (Biorad, Hercules, CA). ^{1}H-T_1 were determined on the Stelar Spinmaster spectrometer (Stelar, Mede, Italy) operating at 21.5 MHz. ^{157}Gd enriched Gd_2O_3 oxide (92.3 %) was purchased by Trace sciences international (Canada). Hydrated mean diameters of AT101/LDL particles were measured by a dynamic light scattering spectrophotometer (Malvern Zetasizer 3000HS). All samples were examined at 25°C in filtered PBS (phosphate-buffered saline) buffer (pH 7).

2.2 Cell Lines. Mouse mesothelioma (AE17) cell line was obtained from Sigma Aldrich and it was cultured in RPMI medium (Lonza) supplemented with 25mM Hepes, 5% (v/v) FBS (fetal bovine serum) and 2mM glutamine. Human mesothelioma (ZL34) cell line was obtained from Sigma Aldrich and it was cultured in DMEM-Ham's F12 (Lonza) containing 2.5 mM glutamine and supplemented with 15% (v/v) FBS. NMuMg cell line, derived from a healthy mouse mammary gland (kindly provided by Prof. Lollini PL, University of Bologna), was cultured in RPMI (Lonza) contained 4mM glutamine, supplemented with 10% FBS and 10 µg/ml human insulin (Sigma). MRC−5 cell line (healthy human lung fibroblasts) was obtained from ATCC (Manassas, Virginia, USA) and they were cultured in EMEM medium (Lonza) supplemented with 10% (v/v) FBS, 2 mM glutamine, 1 mM sodium pyruvate and nonessential amino acids. All media contained 100 U/ml penicillin and 100 U/ml streptomycin. All cell lines were maintained in a humidified incubator at 37°C, 5% CO_2.

2.3 Uptake Experiments. For the *in vitro* uptake experiments, 4.5 x 10^5 AE17, 4.5 x 10^5 ZL34, 2 x 10^5 MRC−5 and 2 x 10^5 NMuMg were seeded in 6 cm diameter dishes. After 6 hours, the cells were incubated for 24 hours with the respective culture media supplemented with LPDS (Lipoprotein Deficient Serum, Biomedical Technologies Inc., Stoughton, MA) to increase LDLR expression. Finally, the cells were incubated for 16 hours with AT101 loaded LDL particles (AT101/LDL) at concentrations ranging from 5 to 50 µg/ml. For competition assays, AT101/LDL particles were incubated in the presence of 200 µg/ml native LDL. At the end of the incubation, cells were washed three times with PBS, detached with trypsin/EDTA (ethylenediaminetetraacetic acid). AE17 and ZL34 cells were also transferred into glass capillaries for MRI analysis (see below). Then AE17, ZL34, MRC−5 and NMuMg cells were

suspended in 200ul of PBS, sonicated for 30” at 30% power in ice and their protein concentration was measured by the Bradford method, using BSA (bovine serum albumin) as standard. Boron and Gd amount in each cell sample was evaluated by ICP-MS. Digestion was performed by heating under microwave 0.2 ml of cell suspensions for 20’ at 160°C, after the addition of 1 ml of concentrated HNO_3 (70%). After mineralization, 3 ml of ultrapure water were added to the remaining sample volumes for ICP-MS analysis.

2.4 FACS analysis of LDL Receptor expression. In order to perform FACS (Fluorescence Activated Cell Sorting) analysis, 4.5 $x10^5$ AE17, 4.5 x 10^5 ZL34, 2 x 10^5 MRC−5 and 2 x 10^5 NMuMg cells were seeded in T25 flasks. After 6h, the cells were incubated for 24 hours with the respective culture media supplemented with LPDS. Then, the LPDS medium was renewed for other 16h. Finally, the cells were washed with PBS. They were detached with trypsin/EDTA, transferred in 15 ml falcon tubes and counted in PBS. Cell number was determined using a cell sorting chamber (Burker-Turk chamber). AE17, ZL34, MRC−5 and NMuMg cells were divided in 3 falcon tubes containing $1x10^6$ cells. (Sample 1: no antibody incubated; sample 2: secondary antibody incubated; sample 3: primary and secondary antibodies incubated). All cells were fixed with 4% paraformaldehyde (7 min, 1 ml); then 2 ml of PBS were added to the cells before centrifugation (1100 rpm for 5’). After a further washing with 3 ml of PBS, cells were permeabilized with 0.1% (v/v) of Tween20 in PBS (20 min, 1 ml); then 2 ml of PBS were added to the cells and they were centrifuged (1100 rpm for 5’); the PBS was removed and the cells were further washed with 3 ml of PBS and centrifuged (1100 rpm for 5’). All the cells were then incubated at 4°C in 10% FBS (v/v) in PBS (10 min, 1 ml) to block non−specific protein−protein interaction. Then 2 ml of PBS were added to the cells and they were centrifuged (1100 rpm for 5’); After a further washing with 3ml of PBS the primary anti−LDL receptor

monoclonal antibody (Abcam ab52818) was incubated 30 min at 4°C to cell samples n° 2 (3 µl in 200ul of 0.1% BSA/PBS). Then 3 ml of PBS were added to the cells and they were centrifuged (1100 rpm for 5'); the PBS was removed and the cells were further washed with 3 ml of PBS and centrifuged (1100 rpm for 5'). Then, a swine anti−rabbit secondary antibody FITC-conjugated (Dako F0205) (3ul in 200ul of 0.1% BSA/PBS) was incubated to samples 2 and 3. The incubation was performed at 4 °C for 30'. All samples were washed with PBS (2 × 3 ml) and centrifuged (1100 rpm for 5'). Finally, all the cells were diluted in PBS (250µl) and evaluated for their FITC fluorescence on a flow cytometer (Becton Dickinson, FACS Calibur). Their FITC fluorescence (geo mean fluorescence intensity) was analyzed using the CELLQUEST PRO program.

2.5 Experimental Mice and Induction of Transplantable Tumors. 6 week old female Nu/Nu nude mice (n=15) were purchased from Charles River Laboratories (Calco, Italy) and maintained in specific pathogen free conditions at the Department of Molecular Biotechnology and Heath Sciences of the Turin University, Italy. Their handling and manipulations were performed according to European Community guidelines, and all the experiments were approved by the Ethical Committee of the University of Turin. ZL34 cell lines were cultured as described above and subcutaneous mesothelioma tumors model developed after the injection of 6 x 10^6 cells in 0.15ml (1:1 Matrigel: PBS). The ZL34 tumors grew quite quickly and after 12-15 days they had reached a volume of 70±20 mm^3.

2.6 MRI. *In vitro* experiments: about 3 x10^6 AE17 cells and 2 x 10^6 ZL34 cells were collocated in glass capillaries inside an agar phantom and MR images were acquired using a standard T_1-weighted multi slice spin-echo sequence (TR (repetition time)/TE (echo time)/NEX number of

excitations) = 250/3.7/6, FOV (field of view) = 1.2 cm) on a Bruker Avance300 spectrometer (7 T) provided with a Micro 2.5 microimaging probe (Bruker BioSpin, Ettlingen, Germany). T_1 relaxation times were determined using a standard Saturation Recovery Spin Echo. *In vivo* experiments: before MRI acquisition, animals (n=5) were anesthetized by injecting tiletamine/zolazepam (Zoletil 100; Virbac, Milan, Italy) 20 mg/kg + xylazine (Rompun; Bayer, Milan, Italy) 5 mg/kg. AT101/LDL particles were injected via tail vein at a dose of 0.1 mmol Gd/kg. MR images at 7 T were acquired before and after 3, 5 and 24 h AT101/LDL administration using a T_1-weighted, fat-suppressed, spin-echo sequence (TR/TE/NEX=250:3.4:8, FOV=2.8 cm). The T_1 relaxation times of the different organs in the PRE contrast images were acquired using a SNAP sequence (TR/TE/NEX=3.4:1.3:16). The mean signal intensity (SI) values were determined in the regions of interest (ROI) manually drawn on the muscle, liver and the whole tumor, in all time intervals considered. The mean measured SI was normalized using a tube containing standard Gd solution. The mean SI enhancement (% enhancement) of target tissues was calculated in accordance with the following equation:

$$\text{SI \% Enhancement} = ((\text{mean } SI_{POST} - \text{mean } SI_{PRE}) / \text{mean } SI_{PRE}) \times 100$$

Tumor volumes were calculated from T_2-weighted MR images by a RARE sequence protocol (TR/TE/NEX=2500:50.2:6 FOV=4.0 cm) at 1 T with an Aspect M2-High Performance MRI System (Aspect Magnet Technologies Ltd., Netanya, Israel) consisting of a NdFeB magnet, provided with a 35 mm solenoid Tx/Tr coil of inner diameter 35 mm. The system is supplied with fast gradient coils (gradient strength, 450 mT m^{-1} at 60 A; ramp time, 250 μs at 160 V) with a field homogeneity of 0.2−0.5 gauss.

2.7 Gd and Boron concentration determination by MRI. By using equation 1, the concentration of Gd and Boron atoms were determined from R_{1POST} and R_{1PRE} relaxation rates.

$$[B]\ \mu g/g = 100 \times (R_{1POST}-R_{1PRE})/ r_{1p(incell)}$$

Eq. 1

where r_{1p}(in cell) is the intracellular relaxivity of AT101/LDL (3.6 mM^{-1} s^{-1} at 7 T) [22]. This value is similar to the adduct relaxivity measured in buffer solution at 7T (3.7 mM^{-1} s^{-1}, T=25°C).

The R_1 PRE-contrast (R_{1pre}) maps were obtained by using a SNAP sequence; R_1 POST-contrast (R_{1POST}) maps were calculated by using the pre- and post-contrast SI ratio (Eq. 2) calculated in the regions of interest, which were manually drawn on T_1-weighted images:

$$\frac{SI_{PRE}}{SI_{POST}} = \frac{\{[1-exp(-TR-TE)R1_{PRE}]\}\exp(-TExR2)}{\{[1-exp(-TR-TE)R1_{POST}]\}\exp(-TExR2)} \qquad \text{Eq. 2}$$

In Equation 2 [25], TR is the repetition time, TE is the echo time, and R_1 and R_2 are the water proton relaxation rates.

2.8 Mice Irradiation. Mice models were generated by the injection of 6 x 10^6 ZL34 cells in 0.15 ml (1:1 Matrigel: PBS) in the neck of the mouse two weeks before the treatment. Animal irradiations were performed in the thermal column of the TRIGA Mark II reactor at University of Pavia (Italy). The irradiation facility was previously designed for TAOrMINA treatment developed to treat multiple liver metastases with BNCT [26]. The chamber used to perform animal irradiation has a cross section of 40 × 20 cm^2, a length of 1 m and it starts at about 1.3 m

from the centre of the reactor core. The animal irradiation position has been recently characterized in terms of neutron spectrum and background photon dose [27]. To carry out neutron irradiation animals are positioned at the end of this chamber where the in air thermal neutron flux is approximately 1.2 x 10^{10} n/cm^2s, operating the reactor at its maximum power. In this way the thermal neutron flux is maximized and the irradiation time is kept as short as possible (never longer than 15 minutes). The first mice group (n=5) received AT101/LDL (1 mmol boron/kg dose) 5 hours before irradiation. Group two (irradiated control group, n=5) received at the same time, the same volume of PBS. As the neutron field of the TRIGA Mark II is not collimated, the whole body of the animal is exposed to the neutron field during the irradiation. In order to reduce neutron exposure of healthy organs, a shield made of 95% ^{6}Li-enriched Li_2CO_3 powder was used as neutron absorber. Lithium-6 is an ideal isotope to build effective neutron shields for in vivo experiments thanks to the absence of secondary gamma radiation after thermal neutron capture. The designing of the treatment plan war carried out using the simulation code Monte Carlo N-Particles (MCNP). The validation of the simulation was performed with neutron flux measurements by the activation of Cu wires using the Westcott formalism [28]. In the experimental protocol used during the irradiation experiments, 5 mice are irradiated at the same time, each mouse was protected by two units of Li_2CO_3 neutron shield to cover the head and the abdomen regions. The units are kept separated of about 1 cm to guarantee the direct exposure of the tumors to the neutron flux.

3. RESULTS

3.1 LDL/AT101 supramolecular adduct synthesis and characterization. The preparation of the dual boron/Gd containing compound (AT101) used in this study (Figure 1) and its LDL adduct was carried out using the previously reported procedures [22]. Briefly as AT101 (Figure 1) is an amphiphilic molecule, it makes large sized micelles in aqueous solution. Thereafter, before the incubation with LDL micelles were disaggregated by the addition of an excess of β-cyclodextrin (β-CD) to disperse the amphiphilic complexes in PBS. Then LDL were added step-wise to the solution of the β-CD/AT101 adduct in order to transfer AT101 complexes from β-CD to LDLs particles. The obtained AT101/LDL adducts showed a thermodynamic association constant (Ka) of 1.7×10^4 M^{-1} and a binding site number of 300 available to AT101 per LDL molecule [22]. The adduct size measured by dynamic light scattering (DLS) was of 24 ± 2 nm. This value was not significantly different from the native LDL particles (23 ± 1 nm). The adduct r_{1p} (the observed relaxation rate of a water solution containing 1 mM of a paramagnetic species) was 15.5 mM^{-1} s^{-1} (20 MHz, 25°C). Moreover, a TEM image confirming the round shape and size of AT101/LDL particle is reported in the supporting information (Figure S1). The stability of AT101/LDL was evaluated by dialyzing the adduct solutions (1.5 ml in a 14000 Da cut−off membrane) in 40 ml of PBS buffer at 37°C for 3 days. Gd, Boron and proteins concentrations were measured at different time intervals (6, 24, 48, and 72 hours) by ICP-MS and Bradford assay, respectively (Figure S2). The measurement of a practically unchanged ratio between Gd, Boron and protein, confirmed the adduct stability over the investigated time interval.

3.2 Evaluation of Low Density Lipoproteins receptors (LDLRs) expression on mesothelioma cell lines. Flow cytometry (FACS) analysis was carried out to evaluate LDLRs expression on the membrane of ZL34 and AE17, human and murine mesothelioma cell

lines, respectively. Cells were incubated 30’ with a monoclonal antibody (mAb) specific for LDLRs and then with the FITC-labeled secondary Ab (FITC=fluorescein isothiocyanate) (Figure 2). Unlabelled cell samples (violet area) were used as control. The secondary Ab aspecific binding was determined incubating cells avoiding pre-incubation with the primary Ab (green line). Anti−LDL receptors mAb yielded a higher positive signal in human ZL34 and in murine AE17 mesothelioma cells with respect to healthy human lung fibroblasts MRC−5 and murine healthy mammary gland NMuMg cells, respectively. This demonstrate a high level of expression of LDLRs in mesothelioma cell lines when compared to healthy cells.

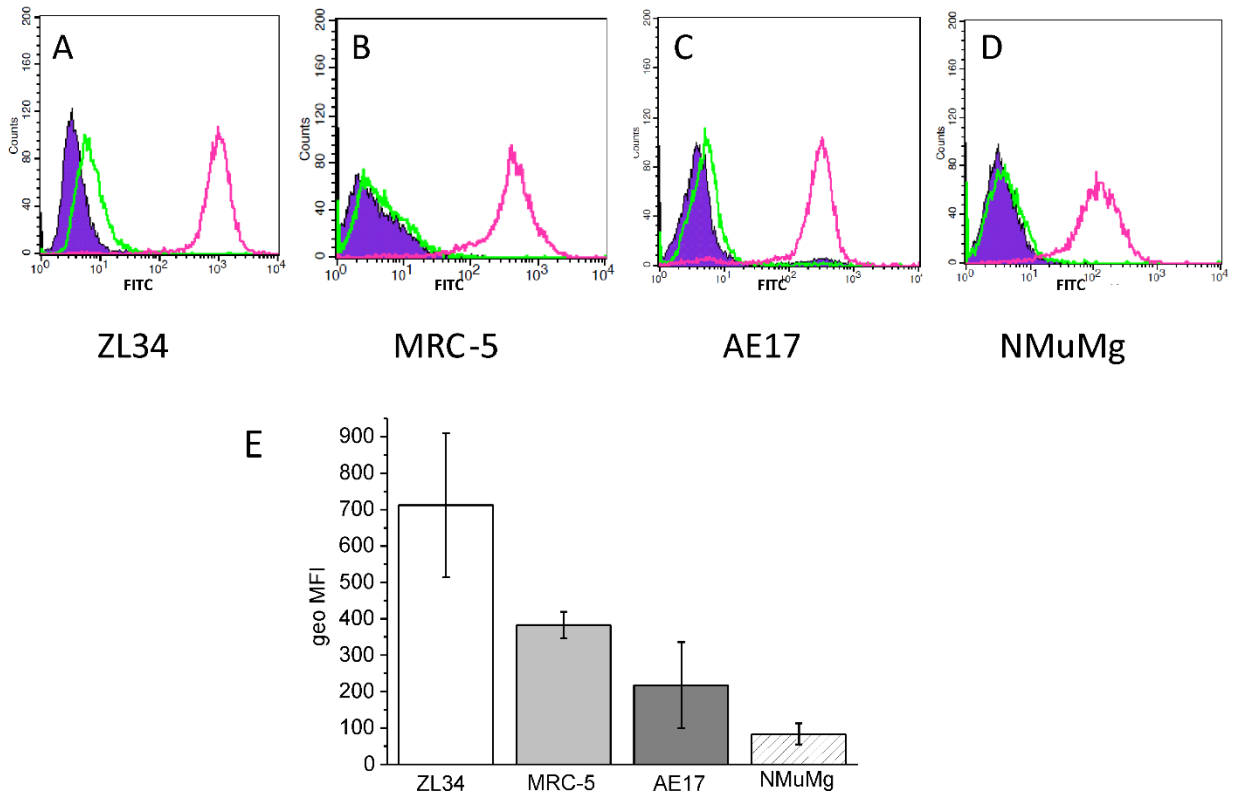

Figure 2: FACS analysis of the LDL receptors expression on ZL34, MRC−5, AE17 and NMuMg cell lines. A, B, C, D panels show the fluorescence intensity of LDL receptors expression on ZL34, MRC−5, AE17 and NMuMg cell lines, respectively. The positivity is defined as fluorescence intensity of FITC (anti−LDL receptor Ab conjugated with FITC

secondary Ab) (pink line) higher than that of the FITC secondary Ab used as control (green line). Untreated cells are shown in violet. E) The geometric mean fluorescence intensity (geo MFI) was analyzed using the CELLQUES PRO program.

3.3 Cell uptake experiments and MRI. In order to evaluate whether the upregulated expression of LDL receptors on the cytosolic membrane of ZL34 and AE17 cell lines can deliver a sufficient amount of boron to perform BNCT, uptake studies were carried out incubating ZL34 and AE17 cells with increasing concentrations of the AT101/LDL for 16 hours at 37°C. Cells were then washed with cold PBS, collected and the Gd and boron contents were measured by ICP-MS analysis. Figure 3 shows that the internalization of Gd (Figure 3A) and boron (Figure 3B) containing AT101/LDL by tumor cells is significantly more efficient than that observed with healthy MRC−5 and NMuMg cells. A LDL concentration of 25 μg/ml (0.107 mM in boron) in the culture medium was sufficient to accumulate into ZL34 and AE17 cells 36 and 18 μg/g of boron, respectively. The attained concentration appears sufficient to pursue a successful treatment.

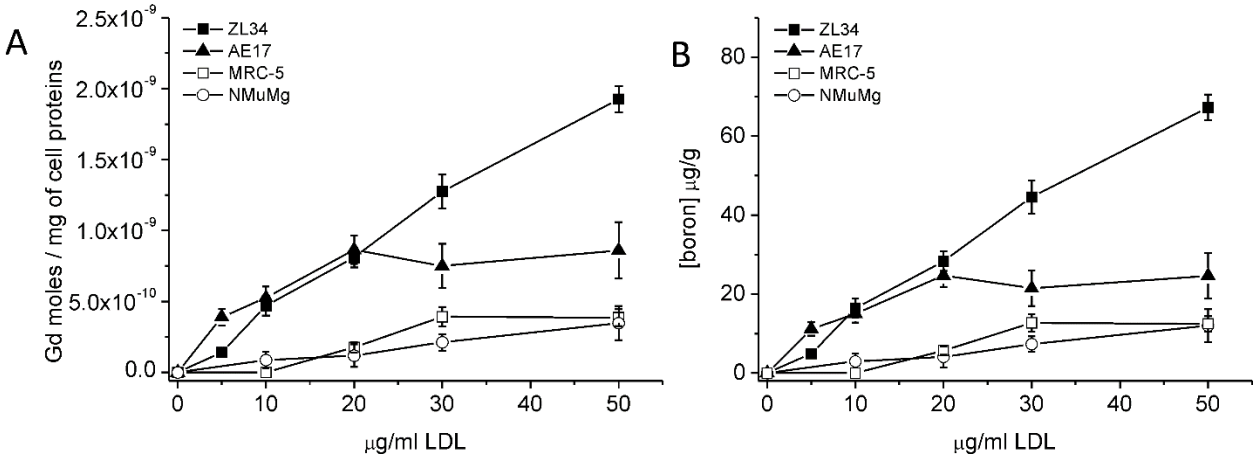

Figure 3: In vitro uptake experiments on ZL34, AE17, MRC−5 and NMuMg cell lines. Cells were incubated for 16 hours at 37 °C in the presence of increasing amounts of AT101/LDL (expressed as protein concentration µg/ml). Gd (A) and boron (B) content in the cell samples was determined by ICP-MS, and values were normalized to the protein content of each cell sample that was correlated to the number of cells by means of a calibration curve: [(mg protein)/ (number of cells)]. The µg of boron per g of tissue were thus calculated considering that 1 g of tissue contains $1x10^9$ cells. Errors bars report the standard deviation (SD) of the data.

The specificity of the AT101/LDL uptake was demonstrated by carrying out competition assays with native LDL (Figure 4). After 16h incubation in the presence of AT101/LDL the uptake by both treated cells decreased of 40% and 60% for ZL34 and AE17, respectively, in the presence of 200 µg/ml native LDL added to the cell medium, thus demonstrating the occurrence of a specific internalization pathway (Figure 4).

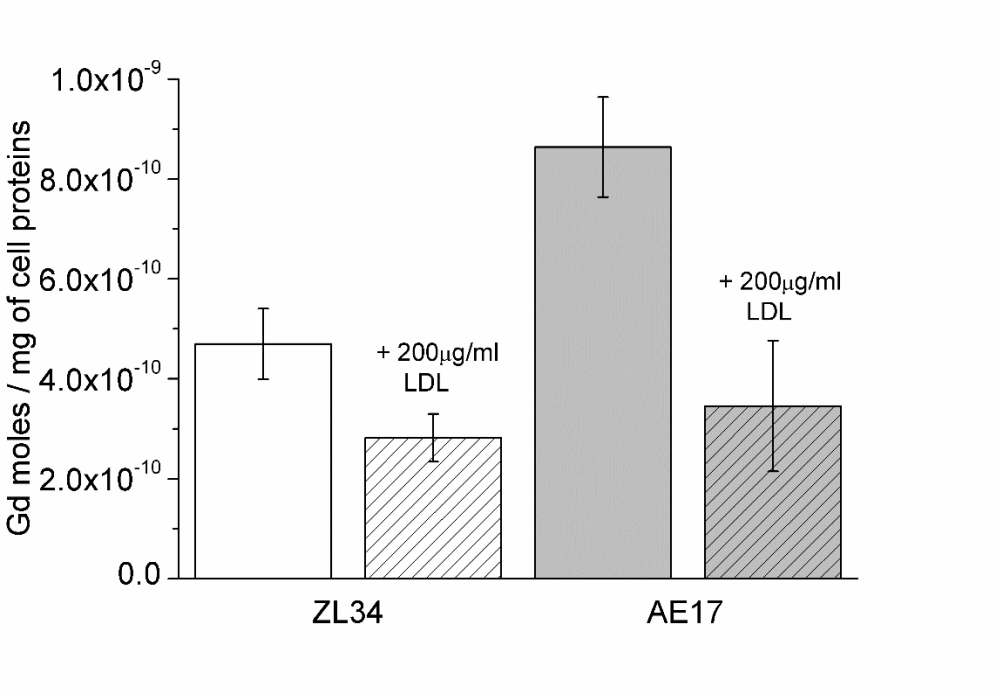

Figure 4: Competition assay performed incubating ZL34 and AE17 for 16 hours at 37°C with 10 and 20 μg/ml of AT101/LDL, respectively, in the absence and in the presence of 200 μg/ml of native LDL

Moreover, T_1 weighted MRI images (7T) were acquired on glass capillaries filled with cell pellets obtained by incubating AE17 and ZL34 cells with 50 μg/ml AT101/LDL. Figure 5A, unequivocally shows the well detectable signal intensity (SI) enhancement of cells incubated in the presence of AT101/LDL in comparison with the control. The relaxation rates R_1 (Figure 5B) of AE17 and ZL34 are directly proportional to the LDL receptors density as determined in Figure 2 (ZL34>AE17).

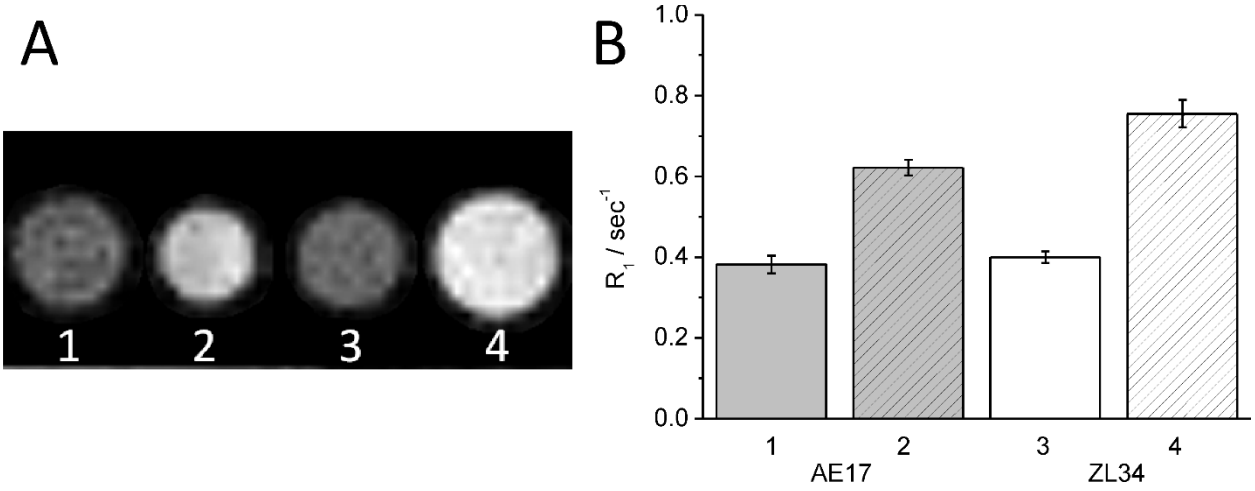

Figure 5: A) T_1-weighted spin-echo MR image of an agar phantom with glass capillaries containing unlabeled AE17 (1) and ZL34 (3) cells and cells incubated with 50 μg/ml of AT101/LDL (2 and 4 for AE17 and ZL34, respectively) for 16 hours at 37°C. B) Relaxation rates (R_1) measured on cell pellets for unlabeled control AE17 (1) and ZL34 cells (3) and cells incubated with 50 μg/ml of AT101/LDL (2 and 4, for AE17 and ZL34, respectively).

3.4 Evaluation of the AT101/LDL particle uptake in transplanted mesothelioma tumors. Since ZL34 human mesothelioma cell line showed the higher expression of LDLR, tumor xenografts were prepared by subcutaneous injection of ca. 6 million ZL34 on Nu/Nu nude mice. After 12-15 days, the ZL34 tumors reached a volume of approximately 70±20 mm^3. At that time, the tumor-bearing mice (n=5) intravenously received a bolus of AT101/LDL at a dose of 0.1 mmol/kg and 1 mmol/kg as expressed in terms of Gd and boron content, respectively. T_1-weighted spin-echo MR-images were acquired before and 3, 5, and 24 hours after AT101/LDL administration. Figure 6 shows representative examples of mesothelioma axial T_1-images acquired before and 3 hours after AT101/LDL administration

(Figure 6A and 6B, respectively). Figure 6C reports the mean SI enhancement (%) measured at the different time intervals. High % SI enhancement are observed in the tumor region and in the liver as a consequence of the high expression of LDL receptors on both tumor cells and normal hepatocytes. Therefore, mice abdomens were protected with a neutron shield during BNCT treatment.

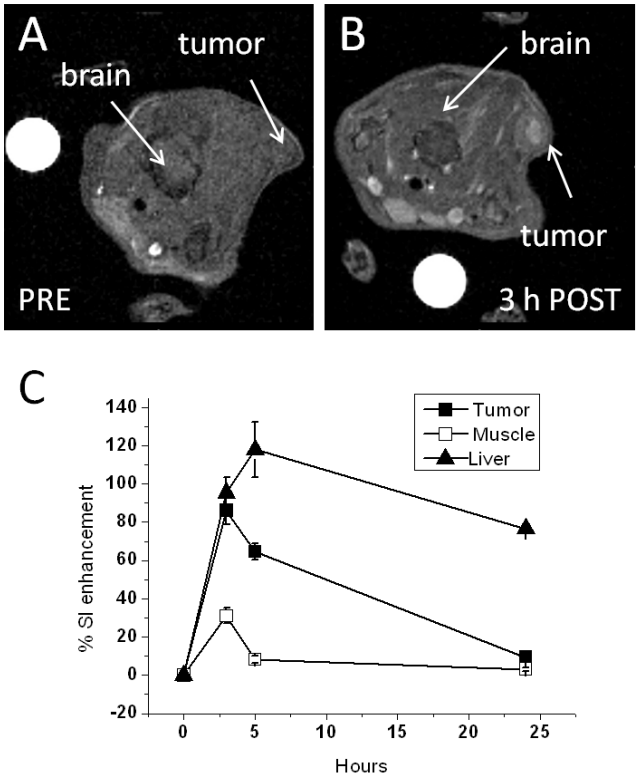

Figure 6: Representative T_1−weighted MR images of Nu/nu nude mice with subcutaneous mesothelioma tumor acquired before (A) and 3h after (B) administration of 1 mmol of boron per kg dose of AT101/LDL nanoparticles. (C) A plot of MRI SI enhancements (%) measured in different organs vs. time after the administration of the AT101/LDL adduct. Error bars report the SD.

The boron concentrations in the mesothelioma tumor xenograft and in the surrounding muscle (Table 1) were calculated at 3, 5 and 24 hours post-injection on the basis of the relationship between the Gd-induced relaxation enhancement and local AT101/LDL concentration. (see Methods)

Table 1. Biodistribution of boron atoms in mesothelioma tumors bearing mice

Time POST i.v.	Tumor[boron] µg/g	Muscle[boron] µg/g	Liver[boron] µg/g	Ratio of boron atoms in Tumor/Muscle
3h	36±3	15±1	69±5	2.4:1
5h	26±2	3.5±0.5	94±13	7.4:1
24h	3±1	1±0.4	52±4	3:1

The intra-tumor boron concentration measured 5h after the AT101/LDL injection resulted suitable for undertaking the BNCT treatment. In fact, at this time, the high boron concentration in tumor (26µg/g) is combined with a high tumor/muscle boron ratio that is of fundamental importance to significantly reduce healthy tissues damage.

3.5 BNCT treatment of subcutaneous model of human mesothelioma. Two groups of animals underwent the irradiation treatment. The first group (irradiated and treated, n=5) received AT101/LDL at a Gd dose of 0.1 mmol/kg corresponding to a boron dose of 1 mmol/kg, five hours before neutron exposure. To assess the aspecific effect of neutron

irradiation (in the absence of AT101/LDL) a second mice group (irradiated control group, n=5) received the same volume of PBS. T_2-weighted RARE images have been acquired to monitor the tumor size by MRI using. In the days after BNCT, a significant tumor size reduction was observed for irradiated and treated group with respect to irradiated control group. (Figure 7)

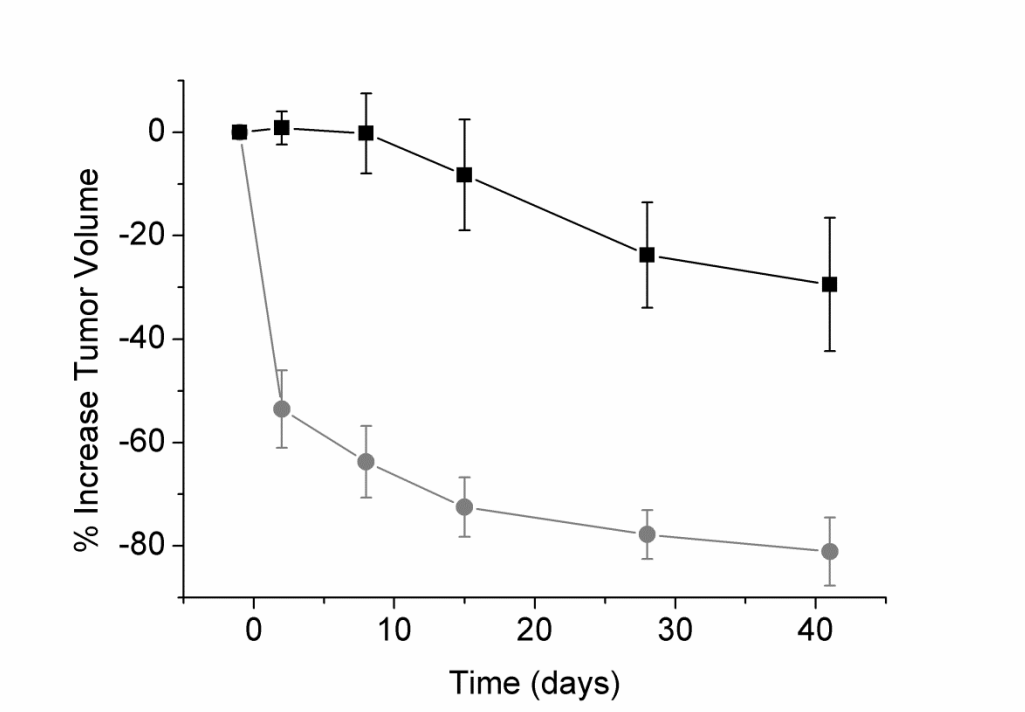

Figure 7: Tumor-growth evaluation performed after neutron irradiation. The graph shows the % increase tumor volume measured by MRI on irradiated control mice (black squares) and irradiated and AT101/LDL treated mice (gray circles). Error bars indicate the SD.

The potential toxicity related to the therapeutic protocol was evaluated by monitoring over time body weights of the two irradiated mice groups. A body weight reduction, reaching the maximum of -10%, was observed during the first 5 days after neutrons irradiation (Figure S3). Then, the original weight was almost fully recovered in the following 5-10 days for both irradiated controls and Boron treated animals."

4. DISCUSSION

The general aim of this work is to establish a new theranostic (therapeutic and diagnostic) approach for the treatment of MM, a rare and aggressive malignancy of the pleura, associated to asbestos exposure. At present, there is no curative treatment for MM that remains an urgent therapeutic challenge to be faced. The herein developed, new targeted, agent is able to deliver a precisely tailored therapy that can be monitored by *in vivo* imaging. The obtained results appear very promising as they may potentially provide patients affected by this rare disease, with an improved therapeutic option, based on the BNCT treatment. In particular, the herein reported results demonstrate, for the first time, that overexpressed LDL receptors can be successfully exploited to deliver to mesothelioma cells a therapeutic dose of boron (=26 µg/g), significantly higher than in the surrounding healthy tissue (=3.5µg/g). Since, human ZL34 mesothelioma internalized a significantly higher amount of boron with respect to both healthy and murine cells, the human model has been selected for *in vivo* studies. Moreover, the presence of a Gd complex in the BNCT agent allows the boron quantification before starting neutron irradiation. This allows the personalization of the neutron irradiation set-up by using the best protocol optimizing the irradiation time and duration. Although also the irradiated control mice group (irradiated without boron administration) showed a slight reduction of tumor volume, the irradiated and treated group showed a drastic reduction of tumor mass of about 80-85%, 40 days after the irradiation. Another interesting observation is the absence of any tumor recurrence until day 40 post-treatment (end point of the experiment) conversely to what observed on melanoma and breast adenocarcinoma metastasis treated with the same boron carrier AT101/LDL [22,23]. This finding could be the consequence of a higher sensitivity of mesothelioma to neutron irradiation.

On the basis of the available literature [29,30] most important tissues at risk in the pleural mesothelioma radiation therapy are skin and healthy lung tissue, while the involvement of other organs such as spinal cord, colon, etc. strictly depends on the peculiar characteristics of each treated clinical case. The lung parenchima is a well known highly radiosensitive tissue, while the skin suffers from two main reasons: i) the high boron absorption by skin (50% higher than the other healthy tissues) together with an high compound biological effectiveness (CBE) factor of 2.5 (value used by almost all the BNCT clinical trials); ii) the physics of the neutron attenuation by superficial tissues and the significant effect of backscattering after the thermalisation of the incident epithermal beam occurring at 1.5-2 cm under the skin surface. This effect increases the net thermal flux irradiating the skin thus inducing a higher amount of capture reaction in boron. Skin radiotoxicity can be reduced by using multiple beams with varying entrance directions, thus spreading the absorbed dose over a wider surface. For healthy lungs, there is a widespread opinion that actually BNCT can guarantee a steep dose gradient, thanks to the selective intratumour boron distribution, which allows killing of cancer cells while remaining below tolerance doses in the healthy parenchima. Such selective treatment is absolutely impossible to be achieved by a conventional external beam radiotherapy. The side effects reported in the literature after a whole lung irradiation by X-rays, neutrons or boron + neutrons are principally radio-induced pneumonitis as acute effect and fibrosis at longer observation times [31,32]. The effective radiation dose able to induce pneumonitis in the 50% of animals (ED50) for X-ray, neutrons alone and BNCT was equals to 11.6, 9.6 and 7.0 Gy, respectively. The absorbed doses [23] calculated in the lung tissues of animals irradiated in the facility used in this study (TRIGA Mark II reactor, Pavia Italy), using the same irradiation time and reactor power (15', 250 kW) yielded a mean value of 3.6 and 1.9 Gy with and without boron administration, respectively.

These values are well below the suggested thresholds [31,32]. Moreover, the absence of any significant side effect, on both mice groups used in this study, confirms what already reported by other authors performing BNCT of mesothelioma mouse models [33,34] i.e. the peculiar BNCT selectivity which is capable of delivering microscopic hot spots of high doses only at the tumour cells while sparing the surrounding healthy tissues thus offering an effective treatment also for diffused or highly infiltrating tumours such as mesothelioma.

One may conclude that BNCT seems to be a treatment particularly efficient on this rare pathology especially when the therapeutic boron is delivered to the tumor cells at high concentrations with high selectivity. These encouraging results could take on an even more important significance as, thanks to the new neutron sources based on proton accelerators, new BNCT centers are being set up directly in hospitals [35].

Acknowledgements.

This work was supported by Italian National Institute of Nuclear Physics project NeTTuNO and it was performed in the framework of the Consorzio Interuniversitario di Ricerca in Chimica dei Metalli dei Sistemi Biologici (CIRCMSB) and of the COST action 15209 (Eurelax).

REFERENCES

[1] J.P. van Meerbeeck, A. Scherpereel, V.F. Surmont, P. Baas, Malignant pleural mesothelioma: the standard of care and challenges for future management, Crit. Rev. Oncol. Hematol 78 (2011) 92–111.

[2] O.D. Røe, G.M. Stella, Malignant pleural mesothelioma: history, controversy and future of a manmade epidemic, Eur. Respir. Rev. 24 (2015) 115–31.

[3] S. Lagniau, K. Lamote, J.P. van Meerbeeck, K.Y. Vermaelen, Biomarkers for early diagnosis of malignant mesothelioma: Do we need another moonshot?, Oncotarget 8 (2017) 53751-62

[4] S. Tsuji, K. Washimi, T. Kageyama, M. Yamashita, M. Yoshihara, R. Matsuura, T. Yokose, Y. Kameda, H. Hayashi, T. Morohoshi, Y. Tsuura, T. Yusa, T. Sato, A. Togayachi, H. Narimatsu, T. Nagasaki, K. Nakamoto, Y. Moriwaki, H. Misawa, K. Hiroshima, Y. Miyagi, K. Imai, HEG1 is a novel mucin-like membrane protein that serves as a diagnostic and therapeutic target for malignant mesothelioma, Sci. Rep. 7 **(**2017**)** 45768.

[5] S.C. Baetke, T. Lammers, F. Kiessling, Applications of nanoparticles for diagnosis and therapy of cancer, Br. J. Radiol. 88 (2015) 20150207.

[6] S. Stanley, Biological nanoparticles and their influence on organisms, Curr. Opin. Biotechnol. 28 (2014**)** 69-74.

[7] L. Li, L. Zhang, M. Knez, Comparison of two endogenous delivery agents in cancer therapy: Exosomes and ferritin, Pharmacol. Res. 110 (2016) 1-9.

[8] C.S. Thaxton, J.S. Rink, P.C. Naha, D.P. Cormode, Lipoproteins and lipoprotein mimetics for imaging and drug delivery, Adv. Drug Deliv. Rev. 106 (2016) 116-131.

[9] S. Geninatti Crich, S. Lanzardo, D. Alberti, S. Belfiore, A. Ciampa, G.B. Giovenzana, C. Lovazzano, R. Pagliarin, S. Aime, Magnetic resonance imaging detection of tumor cells by targeting low-density lipoprotein receptors with Gd-loaded low-density lipoprotein particles, Neoplasia 9, (2007) 1046-56.

[10] N.S. Hosmane, J.A. Maguire, Y. Zhu, M. Takagaki, Boron and gadolinium neutron capture therapy for cancer treatment, World Scientific Publishing Co. Pte. Ltd, Singapore, 2012.

[11] H.R. Mirzaei, A. Sahebkar, R. Salehi, J.S. Nahand, E. Karimi, M.R. Jaafari, H. Mirzaei, Boron neutron capture therapy: Moving toward targeted cancer therapy, J. Cancer Res. Ther. 12 (2016) 520-5.

[12] M. Sasai, H. Nakamura, N. Sougawa, Y. Sakurai, M. Suzuki, C.M. Lee, Novel Hyaluronan Formulation Enhances the Efficacy of Boron Neutron Capture Therapy for Murine Mesothelioma, Anticancer Res. 36 (2016) 907-11.

[13] M. Suzuki, Y. Sakurai, S. Masunaga, Y. Kinashi, K. Nagata, A. Maruhashi, K. Ono, Feasibility of boron neutron capture therapy (BNCT) for malignant pleural mesothelioma from a viewpoint of dose distribution analysis, Int. J. Radiat. Oncol. Biol. Phys. 66 (2006) 1584−9.

[14] W.A.G. Sauerwein, A. Wittig, R. Moss, Y. Nakagawa, Neutron Capture Therapy, Principles and Applications, Springers−Verlag, Berlin Heidelberg, 2012.

[15] R.F. Barth, M.G. Vicente, O.K. Harling, W.S. 3rd Kiger, K.J. Riley, P.J. Binns, F.M. Wagner, M. Suzuki, T. Aihara, I. Kato, S. Kawabata, Current status of boron neutron capture therapy of high grade gliomas and recurrent head and neck cancer, Radiat. Oncol. 7 (2012) 146.

[16] R.F. Barth, Boron neutron capture therapy at the crossroads: challenges and opportunities, Appl. Radiat. Isot. 67 (2009) S3-6.

[17] S. Geninatti-Crich, A. Deagostino, A. Toppino, D. Alberti, P. Venturello, S. Aime, Boronated compounds for imaging guided BNCT applications, Anticancer Agents Med. Chem. 12 (2012) 543-53.

[18] J.F. Valliant, K.J. Guenther, A.S. King, P. Morel, P. Schaffer, O.O. Sogbein, K.A. Stephenson, The medicinal chemistry of carboranes, Coord. Chem. Rev. 232 (2002) 173-230.

[19] G. Wu, R.F. Barth, W. Yang, R. Lee, W. Tjarks, M.V. Backer, J.M. Backer, Boron Containing Macromolecules and Nanovehicles as Delivery Agents for Neutron Capture Therapy, Anti Cancer Agents in Med. Chem. 6 (2006) 167-84.

[20] V. Šícha, P. Farràs, B. Štíbr, F. Teixidor, B. Grüner, C. Viñas, Syntheses of C-substituted icosahedral dicarboranes bearing the 8-dioxane-cobalt bisdicarbollide moiety, J. Organomet. Chem. 694 (2009) 1599-1601.

[21] A.N. Ay, H. Akar, A. Zaulet, C. Vinas, F. Teixidor, B. Zumreoglu-Karan, Carborane-layered double hydroxide nanohybrids for potential targeted- and magnetically targeted-BNCT applications, Dalton Trans 46 (2017) 3303−10.

[22] S. Geninatti-Crich, D. Alberti, I. Szabo, A. Deagostino, A. Toppino, A. Barge, F. Ballarini, S. Bortolussi, P. Bruschi, N. Protti, S. Stella, S. Altieri, P. Venturello, S. Aime, MRI-guided neutron capture therapy by use of a dual gadolinium/boron agent targeted at tumor cells through upregulated low-density lipoprotein transporters, Chemistry 17 (2011) 8479-86.

[23] D. Alberti, N. Protti, A. Toppino, A. Deagostino, S. Lanzardo, S. Bortolussi, S. Altieri, C. Voena, R. Chiarle, S. Geninatti Crich, S. Aime, A theranostic approach based on the use of a dual boron/Gd agent to improve the efficacy of Boron Neutron Capture Therapy in the lung cancer treatment, Nanomedicine 11 (2015) 741-50.

[24] S. Aime, A. Barge, A. Crivello, A. Deagostino, R. Gobetto, C. Nervi, C. Prandi, A. Toppino, P. Venturello, Synthesis of Gd(III)-C-palmitamidomethyl-C'-DOTAMA-C(6)-o-carborane: a new dual agent for innovative MRI/BNCT applications, Org Biomol Chem 6 (2008) 4460-6.

[25] L. Shiftan, T. Israely, M. Cohen, V. Frydman, H. Dafni, R. Stern, M. Neeman, Magnetic resonance imaging visualization of hyaluronidase in ovarian carcinoma, Cancer Res. 65, (2005) 10316-23.

[26] A. Zonta, T. Pinelli, U. Prati, L. Roveda, C. Ferrari, A.M. Clerici, G. Mazzini, P. Dionigi, S. Altieri, S. Bortolussi, P. Bruschi, F. Fossati, Extra-corporeal liver BNCT for the treatment of diffusemetastases: what was learned and what is still to be learned, Appl. Radiat. Isot. 67 (2009) S67-75.

[27] S. Bortolussi, N. Protti, M. Ferrari, I. Postuma, S. Fatemi, M. Prata, F. Ballarini, M.P. Carante, R. Farias, S.J. Gonzã¡lez, M. Marrale, S. Gallo, A. Bartolotta, G. Iacoviello, D. Nigg, S.

Altieri, Neutron flux and gamma dose measurement in the BNCT irradiation facility at the TRIGA reactor of the University of Pavia. NIM-B 414 (2018) 113-120.

[28] N. Protti, S. Manera, M. Prata, D. Alloni, F. Ballarini, A. Borio di Tigliole, S. Bortolussi, P. Bruschi, M. Cagnazzo, M. Garioni, I. Postuma, L. Reversi, A. Salvini, S. Altieri, Gamma residual radioactivity measurements on rats and mice irradiated in the Thermal Column of a TRIGA Mark II reactor for BNCT, Health Phys. 107 (2014) 534-41.

[29] M. Suzuki, O. Suzuki, Y. Sakurai, H. Tanaka, N. Kondo, Y. Kinashi, S. Masunaga, A. Maruhashi, K. Ono, Reirradiation for locally recurrent lung cancer in the chest wall with boron neutron capture therapy (BNCT), Int. Canc. Conf. J. 1 (2012) 235-238.

[30] R.O. Farias, S. Bortolussi, P.R. Menendez, S.J. Gonzalez, Exploring Boron Neutron Capture Therapy for non-small cell lung cancer, Phys. Med. 30 (2014) 888-897.

[31] J.L. Kiger, W.S. Kiger, H. Patel, P.J. Binns, K.J. Riley, J.W. Hopewell, O.K. Harling, J.A. Coderre, Effects of boron neutron capture irradiation on the normal lung of rats, Appl. Radiat. Isot. 61 (2004) 969-973

[32] J.L. Kiger, W.S. Kiger, K.J. Riley, P.J. Binns, H. Patel, J.W. Hopewell, O.K. Harling, P.M. Busse, J.A. Coderre, Functional and histological changes in rat lung after boron neutron capture therapy, Radiat Res 179 (2008) 60-69.

[33] T. Andoh, T. Fujimoto, M. Suzuki, T. Sudo, Y. Sakurai, H. Tanaka, I. Fujita, N. Fukase, H. Moritake,, T. Sugimoto, T. Sakuma, H. Sasai, T. Kawamoto, M. Kirihata, Y. Fukumori, T. Akisue, K. Ono, H. Ichikawa, Boron neutron capture therapy as a new approach fro clear cell sarcoma treatment:: trial using a lung metastasis model of CCS, Appl Radiat Isot 106:. 195-201 (2015)

[34] M.Suzuki, Y.Sakurai, S.Masunaga, Y.Kinashi, K.Nagata, A.Maruhashi, K.Ono, A preliminary experimental study of boron neutron capture therapy for malignant tumours spreading in thoracic cavity, Jpn J Clin Oncol 37(4): 245-249 (2007)

[35] A.J. Kreiner, J. Bergueiro, D. Cartelli, M. Baldo, W. Castell, J.G. Asoia, J. Paduloa, J.C. Suárez Sandína, M. Igarzabala; J. Erhardta, D. Mercuri, A.A. Valdaa, D.M. Minskya, M.E. Debraya, H.R. Somacala, M.E. Capoulata, M.S. Herrera, M.F. del Grosso, L. Gagetti, M. Suarez Anzorenaa, N. Canepaa, N. Reala, M. Gund, H. Taccad, Present status of Accelerator-Based BNCT, Rep. Pract. Oncol. Radiother. 21 (2016) 95–101.